Supplementary Information

A versatile gold leaf immunosensor with a novel functionalization strategy based on Protein L and Trastuzumab-modified surface for efficient HER2 detection

Ivana Kundacina*[a], Silvia Schobesberger[b], Stefan Kittler[c], Helena Thumfart[b], Oliver Spadiut[c], Peter Ertl[b], Nikola Knezevic[a], Vasa Radonic*[a]

*corresponding authors: ivana.kundacina@biosense.rs; vasarad@biosense.rs;

[a] University of Novi Sad, BioSense Institute, Dr Zorana Djindjica 1, 21000 Novi Sad, Serbia; ivana.kundacina@biosense.rs; vasarad@biosense.rs; nknezevic@biosense.rs;

[b] TU Wien, Faculty of Technical Chemistry, Getreidemarkt 9, 1060 Vienna, Austria silvia.schobesberger@tuwien.ac.at; helena.thumfart@tuwien.ac.at; peter.ertl@tuwien.ac.at;

[c] TU Wien, Research Division Integrated Bioprocess Development, Institute of Chemical, Environmental and Bioscience Engineering, Gumpendorfer Strasse 1a, 1060 Vienna, Austria; stefan.kittler@tuwien.ac.at; oliver.spadiut@tuwien.ac.at;

Electrochemical characterization of electrodes

Cyclic voltammetry in sulfuric acid was performed on GLE to determine the composition of the electrode surface. CV measurements resulted in a voltammogram, Fig. A.1a, that contains characteristic oxidation and reduction peaks of gold, at 0.85 V and 0.52 V vs. gold RE, respectively. In addition, the voltammogram for GLE showed narrow and sharp peaks, indicating a fast electrochemical reaction and no charge accumulation. In addition, the stability experiments resulted in a stable signal with sharp peaks of iron oxidation and reduction within the redox couple, Fig. A.1b.

In order to study the effective surface area of the GLE and the commercially available Dropsens electrode, a series of experiments were performed with 10 mM potassium ferro/ferricyanide in PBS. The inset of Fig. A.1c presents voltammograms obtained using GLE with different scan rates. Fig. A.1c presents the oxidation and reduction current peaks of the iron redox couple versus the square root of the scan rate where a linear increase can be determined. With increasing scan rate the potential change occurs more rapidly in time, i.e., more energy is transferred to the ions in solution, resulting in a higher current. Similar results were obtained for the Dropsens electrodes, shown in Fig. A.2.

In addition to the electroactive surface, the roughness factor was calculated as the ratio between the geometric and electroactive surfaces of electrodes. Namely, considering that Dropsens and GLE have the same geometric area of the WE equal to 0.12 cm^2, the roughness factor describes the extent of electrode surface participation in the reaction, i.e., contribution to the signal. For GLE the roughness factor was calculated to be 1.3, whereas for the Dropsens electrode, it was 0.58, which indicates that the Dropsens electrode contains other components. This is most likely caused by the organic components in the paste used in screen printing, which do not participate in the reaction on the surface. However, in the case of GLE, this factor is greater than one, which confirms their roughness and large specific surface area. The rough surface properties of GLE were confirmed in our previous study via 3D profile [1]. The results show that the GLE has a larger electroactive surface compared to Dropsens.

In order to test the sensitivity of the GLE, concentrations of 0.5, 1, 5, and 10 mM potassium ferrocyanide/ferricyanide were prepared in 10 mM potassium chloride, 10 mM PBS, and DIW, and EIS was performed (Fig. A.3). The measured impedance decreased with increasing concentration of the

redox couple. As shown in Figs. A.3d and 3e, the Nyquist plots of the redox couple prepared in DIW and 10 mM potassium chloride indicate different solution resistance values since each redox sample concentration has a different real part of the impedance. For the redox couple prepared in 10 mM PBS buffer, the real part of the impedance has similar values for different concentrations. This consistency can be attributed to the properties of PBS, which effectively buffers pH changes.

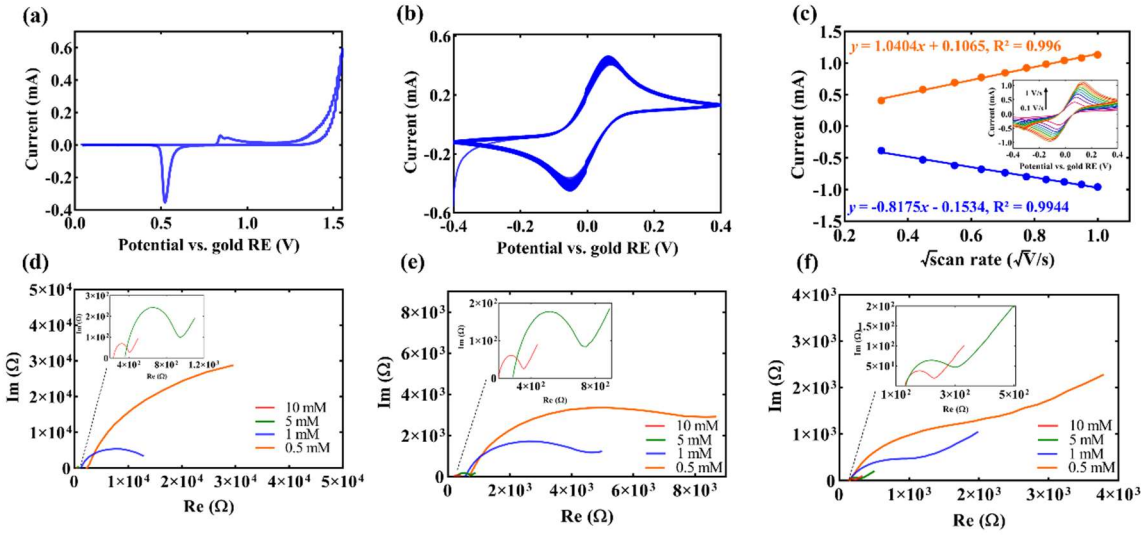

Fig. A.1 Characterization of GLEs; (a) CV of GLE in sulphuric acid; (b) Stability of signal in the redox probe over 100 scans; (c) Oxidation and reduction peaks in the function of square root of scan rate; inset: Voltammograms of the redox probe for scan rates in the range 0.1 – 1 V s^{-1}; (d) Nyquist plots for the redox probe prepared in DIW; inset: 5 mM and 10 mM redox probe; (e) Nyquist plots for the redox probe prepared in potassium chloride; inset: 5 mM and 10 mM redox probe; (f) Nyquist plots for the redox probe prepared in PBS; inset: 5 mM and 10 mM redox probe.

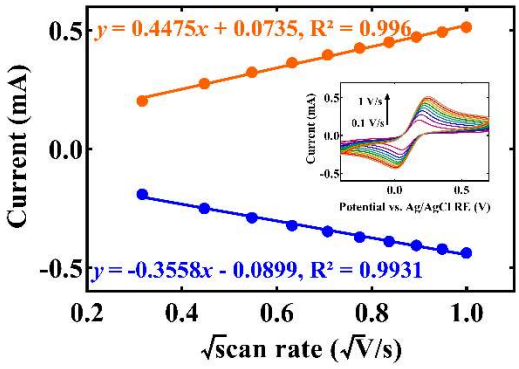

Fig. A.2 Characterization of Dropsens electrode with 10 mM potassium ferro/ferricyanide prepared in PBS; Oxidation and reduction peaks in the function of the square root of scan rate; inset: Voltammograms of redox probe for scan rates in the range 0.1 – 1 V s^{-1}.

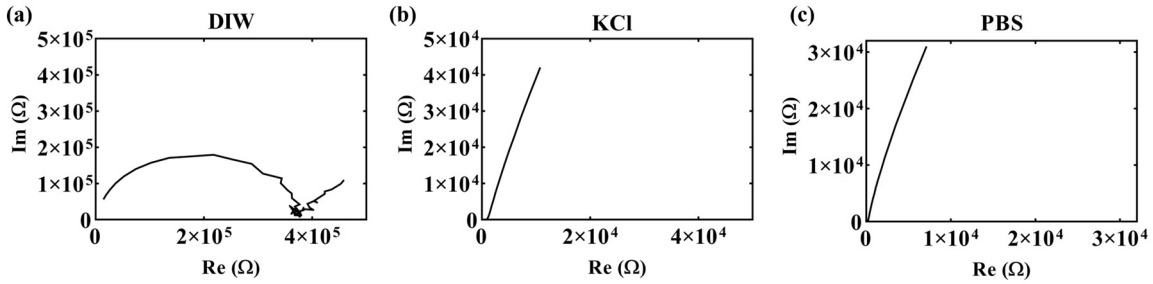

Fig. A.3 (a) Nyquist plots of DIW; (b) 10 mM KCl; (c) 10 mM PBS.

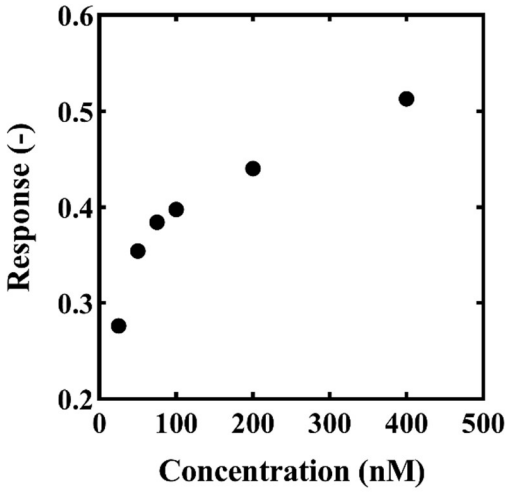

Fig. A.4 Results of the bio-layer interferometry measurement of recombinant protein L.

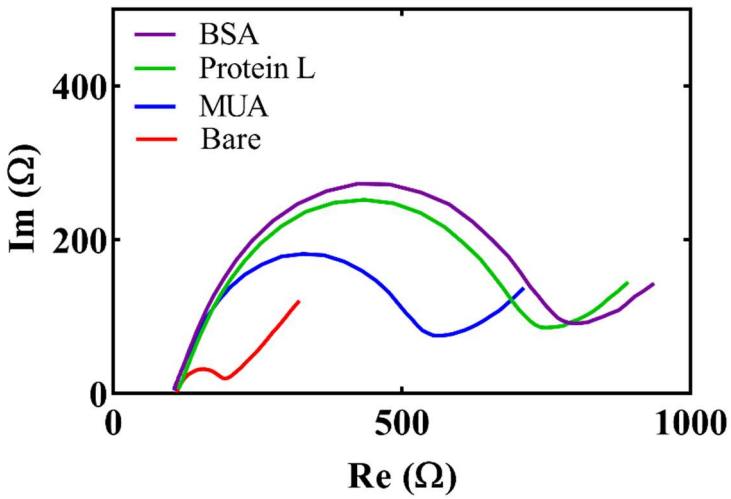

Fig. A.5 Electrochemical characterization of each functionalization step on Dropsens electrode.

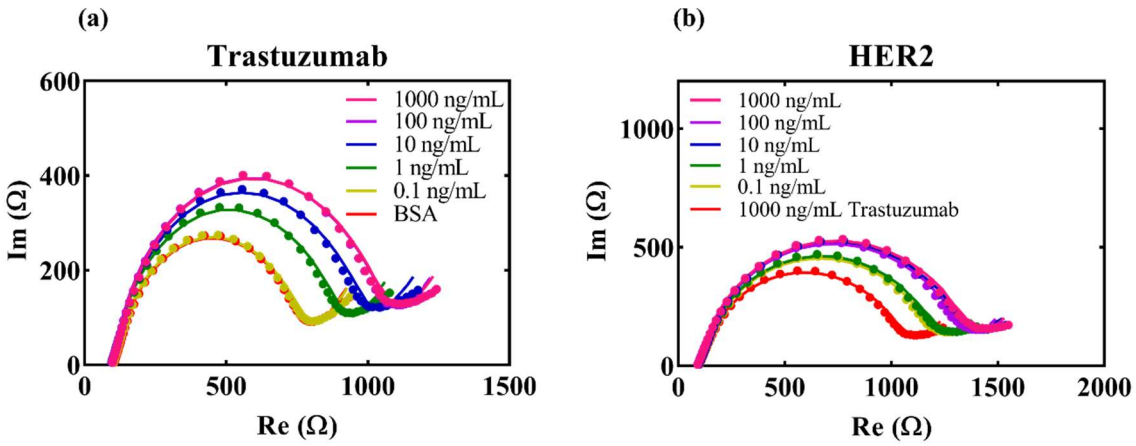

Fig. A.6 Dropsens electrode (a) Nyquist plots for different concentrations of trastuzumab; (b) Nyquist plots for different concentrations of HER2.

Reference:

[1] I. Podunavac, M. Kukkar, V. Léguillier, F. Rizzotto, Z. Pavlovic, L. Janjušević, V. Costache, V. Radonic, J. Vidic, Low-cost goldleaf electrode as a platform for Escherichia coli immunodetection., Talanta. 259 (2023) 124557. https://doi.org/10.1016/j.talanta.2023.124557.